Available online at www.sciencedirect.com

ScienceDirect

journal homepage: www.elsevier.com/locate/he

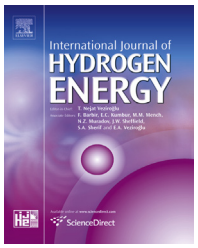

Metagenomic-based analysis of biofilm communities for electrohydrogenesis: From wastewater to hydrogen

Cristiano Varrone [a,1], Joy D. Van Nostrand [b,1], Wenzong Liu [c,**], Benjamin Zhou [b], Zhongshi Wang [b], Fenghai Liu [a], Zhili He [b], Liyou Wu [b], Jizhong Zhou [b], Aijie Wang [a,c,*]

[a] State Key Laboratory of Urban Water Resource and Environment, Harbin Institute of Technology (SKLUWRE, HIT), Harbin, China

[b] Institute for Environmental Genomics and Microbiology and Plant Biology, University of Oklahoma, United States

[c] Research Center for Eco-Environmental Sciences, Chinese Academy of Sciences, Beijing, China

ARTICLE INFO

Article history:
Received 22 August 2013
Received in revised form
26 December 2013
Accepted 3 January 2014
Available online 31 January 2014

Keywords:
Hydrogen
Wastewater
Bioelectrolysis
Biofilm
Functional gene

ABSTRACT

Microbial electrolysis cells (MECs) use exoelectrogenic microorganisms to convert organic matter into H_2, although yields can vary significantly with environmental conditions, likely due to variations in microbial communities. This study was undertaken to better understand how microbial communities affect reactor function. Using wastewater as inoculum, 15 MEC reactors were operated for >50 days and subsequently five reactors were selected for further analysis. Solution (26 mL) was collected every 3–4 days for DNA extraction. DNA was hybridized to GeoChip, a comprehensive functional gene array, to examine differences in the reactor microbial communities. A large variety of microbial functional genes were observed in all reactors. Performances ranged from poor (0.1 ± 0.1 mL) to high (12.2 ± 1.0 mL) H_2 production, with a maximum yield of 5.01 ± 0.43 mol H_2/mol$_{glucose}$. The best performance was associated with higher cytochrome *c* genes, considerably higher exoelectrogenic bacteria (such as *Shewanella*, *Geobacter*), less methanogens and less hydrogen-utilizing bacteria. The results confirmed the possibility to obtain an effective community for hydrogen production using wastewater as inoculum. Not like fermentation, hydrogen production was significantly controlled by electron transporting process in MECs. GeoChip findings suggested that biofilm formation can be highly stochastic and that presence of dissimilatory metal-reducing bacteria and antagonistic methanogens is critical for efficient hydrogen production in MEC reactors.

1. Introduction

It is now largely accepted that the dependence on fossil fuels as our primary energy carrier is contributing to global climate changes, environmental degradation and health problems [1,2]. Renewables are thus gaining more importance as an alternative pollution-free solution for the future, worldwide [3]. The United States, for instance, among the largest energy

* *Corresponding author*. State Key Laboratory of Urban Water Resource and Environment, Harbin Institute of Technology (SKLUWRE, HIT), Harbin, China.
** *Corresponding author*. Tel.: +86 13796629968.
E-mail addresses: liuwz0326@126.com (W. Liu), waj0578@hit.edu.cn (A. Wang).
[1] Authors contributed equally to this manuscript.
0360-3199/$ – see front matter
http://dx.doi.org/10.1016/j.ijhydene.2014.01.001

and fossil fuel consumers, are starting to face several energy-related challenges, such as economic and energy growth, energy security, and climate protection [4]. Because of potential risks to the U.S.'s reliance on fossil fuels (i.e., inability to produce sufficient fuel) there is an urgent need for new sources of renewable energy too. Clearly those are issues of global concern, thus besides the U.S., also the EU, Brazil and China have all launched ambitious programs promoting biofuels in the world [5,6].

Hydrogen (H_2) is one of the most promising emerging energy carriers, because it is clean, efficient, renewable, and has no CO_2 release or toxic bioproducts [7,8]. Thanks to these qualities, H_2 could replace fossil fuels as the next generation energy carrier [9–11].

Several biological processes can produce biohydrogen [10,12], including photosynthesis, dark fermentation [13], and photo fermentation [14]. Biohydrogen production via dark fermentation is one of the most efficient methods (with a stoichiometric potential of 12 mol H_2/mol [15]) and has been intensely studied [10], although the practical yield is relatively low (usually between 2 and 3 mol $H_2/mol_{glucose}$) and results in production of several so-called "dead end" products (i.e., acetate and other fermentation products such as butyrate and alcohols) [15], which cannot be further oxidized through dark fermentation without additional energy input, due to thermodynamic limitations [16,17].

A new alternative process for biohydrogen production is electrohydrogenesis, which uses exoelectrogenic bacteria in microbial electrolysis cells (MECs) able to utilize the dead end products, derived from fermentation, to produce additional hydrogen [7,17] and further oxidize the substrate obtained from the dark fermentation effluent.

Generally, the MEC consists of an anode which accepts electrons from the microbial culture, and a cathode, which transfers electrons to an electron acceptor (proton) under anaerobic conditions [16]. Electrons flow from the anode to the cathode through an external electrical connection. Anode and cathode are typically separated by a semi-permeable membrane, which allows protons released from organic matter to move from the anode to the cathode chamber. At the cathode, electrons and protons combine to form pure H_2, in the presence of a small amount of external voltage [7]. Recently, a single chamber MEC without a membrane has been developed to produce H_2, thus potentially reducing the costs of bioreactor setup and simplifying the bioreactor design. Various experimental results demonstrate that single chamber MECs work well for H_2 production [17–19]. However, while MECs appear to be a promising mechanism for efficient biohydrogen production, these systems still suffer from high variability, and little is known regarding the function of microbial populations involved.

To date, most studies of MECs and microbial fuel cells (MFCs) have investigated the microbial composition, using methods such as 16S rDNA sequencing [20–22] and denaturing gradient gel electrophoresis [23,24]. However, while these methods can provide insight about which bacteria are present, it does not provide information on the microbe's functional abilities.

A recent study examined microbial communities in MFCs and MECs, operated under different conditions, using a comprehensive functional gene array [18]. This study indicated that the functional diversity in all reactors was high, even with acetate as the only carbon source, and that the highest hydrogen yield was associated with the highest abundance of genes involved in complex carbon degradation. GeoChip can thus be used to identify a large variety of geochemically important functional genes (such as carbon-, nitrogen- and sulfur-cycling genes, those related to phosphorous utilization, metal resistance, etc.), which can be used for profiling changes in microbial community functional structures under different conditions [18].

In the present study, we used a comprehensive functional gene array, GeoChip 3.0 [25], to examine functional microbial community differences in single chamber MECs producing different amounts of H_2. The objectives of this study were 1) to develop a suitable microbial community that efficiently produced H_2 using wastewater as inoculum, and 2) to better understand how differences in microbial communities can affect H_2 production.

2. Materials and methods

2.1. Reactor setup and operation

All experiments used polycarbonate single chamber reactors with anodes and cathodes as previously described [16,18]. Each reactor was made of a chamber (28.5 mL) and a gas collection tube (14.5 mL), which was placed at the top of the reactor, and was run in MEC mode with the cathode placed against the sealed wall of the reactor, opposite the anode brush, and applying a fixed voltage of 0.7 V.

Fifteen single chamber reactors were set up and inoculated, using domestic wastewater (primary clarifier effluent) from the Norman Wastewater Treatment Plant (Norman, Oklahoma). The minimal medium contained 50 mM phosphate buffer (pH 7.0; conductivity 7.5 mS cm^{-1}), 310 mg L^{-1} NH_4Cl, 130 mg L^{-1} KCl, a trace nutrient solution (Wolfe's vitamin and mineral solutions), and 1.0 g L^{-1} glucose as the sole carbon source.

At startup, reactors were fed a mixture of equal parts wastewater and buffer solution for two (24-h) batch cycles, and then switched to the glucose medium and operated as MECs for one month. The medium was replaced when the current decreased below 0.2 mA, and the reactors were purged with N_2 (99.998%) for 20 min. Reactors were maintained at room temperature (25 °C).

Gases were collected in gas bags (0.1 L capacity; Cali-5-Bond, Calibrated Instruments) for analysis. Gas samples were collected using a syringe (1 mL, Sample-Lock Syringe) from the reactor headspace and the gasbag. Gas chromatography (Agilent 6890N, with N_2 as a carrier gas) was then used to analyze the gases (H_2, CO_2, CH_4). Voltages across a resistor (1.3 ohms) were measured using a multimeter (model 2700; Keithley Instruments). Glucose content was determined at the start and end of each cycle, using high performance liquid chromatography (HPLC, Agilent 1200).

MECs were operated for 56 days to allow microbial communities and functions to stabilize. Based on reactor functioning, five reactors were selected for further study. Every

2–3 days, 26 mL solution was collected from each reactor, centrifuged (8000 rpm), and the resultant pellets were stored at −80 °C for consequent DNA extraction. Since reactor function had stabilized, samples from days 45, 48, and 52 were used as biological replicates.

2.2. DNA extraction, amplification, labeling and hybridization

DNA was isolated from cell pellets using a freeze-grinding method [26]. DNA (100 ng) from each sample was amplified using the TempliPhi kit (GE Healthcare) following a modified method [27]. Amplified DNA (~2 μg) was labeled with Cy-5 using random priming with Klenow as described previously [28]. Samples were hybridized to GeoChip 3.0 for 12 h at 42 °C and 40% formamide with mixing on a MAUI Hybridization station (BioMicro, Salt Lake City, UT).

2.3. Data analysis

Hybridized GeoChips were scanned (ScanArray Express Microarray Scanner, Perkin Elmer) and digitally analyzed using ImaGene (6.0 premium version, BioDiscovery, El Segundo, CA, USA). Spots with signal-to-noise ratios (SNR) <2, outliers (standard deviation >3), and poor spots were removed. Data normalization was performed as described previously [28,29].

Cluster analysis was performed using the pairwise average-linkage hierarchical clustering algorithm in CLUSTER (http://rana.stanford.edu) and visualized with TREEVIEW (http://rana.stanford.edu/). The majority of analyses were performed using R with functions in vegan packages [30], with some additional code utilizing vegan installed in our GeoChip analysis pipeline (ieg.ou.edu).

3. Results

3.1. Reactor performance

Five sets of reactors (designated as reactors A–E), having differing levels of efficiency (Table 1), were examined. Reactor A was characterized by the highest amount of CH_4 but low H_2 and CO_2 production. Reactor B showed a high production of H_2, CO_2 as well as CH_4. Reactor C obtained the best results, producing the highest amount of H_2 and having the highest CE and CP. Reactor D, instead, had the poorest performance, with little H_2 production and the lowest CE of all reactors. Finally, reactor E had a moderate level of performance. Overall, with the only exception of reactor D, all reactor replicates showed fairly stable performances (Fig. S1), with similar levels of gas production and CE (Table 1). Reactors B, C and E grouped together, with the latter showing a higher variability in terms of H_2 production. Reactor A clearly showed the smallest variability.

Table 2 – Average values of richness, diversity and evenness indexes for each reactor based on GeoChip results.

	Shannon	Simpson	Pielou	SimpsonE
A	6.66 ± 0.51	591.4 ± 251.3	0.96 ± 0.01	0.51 ± 0.02
B	5.07 ± 0.27	107 ± 38.4	0.92 ± 0.02	0.43 ± 0.06
C	5.08 ± 0.08	101.5 ± 17.5	0.92 ± 0.01	0.41 ± 0.06
D	5.74 ± 0.16	208.8 ± 44.9	0.94 ± 0.01	0.47 ± 0.05
E	6.58 ± 0.17	494.9 ± 67.04	0.95 ± 0.01	0.50 ± 0.02

E = Evenness.

3.2. Community functional diversity

Community functional gene diversity, richness, and evenness of each reactor community were assessed, based on GeoChip results (Table 2). Approximately 2000 different functional genes were detected across all reactors, containing from 250 to 1200 genes each. Highest gene numbers (1000–1200) were detected in Reactors A and E, while the lowest gene numbers (~250) were detected in B and C. Highest diversity was also noted for A and E, with B and C having the lowest.

3.3. Community structure differences

To visualize differences in overall functional structure, all genes detected by GeoChip were used for cluster analysis (Fig. 1). All clusters contained a variety of functional genes and in general covered most categories contained on the GeoChip. Cluster 3 genes, for instance, were involved in a variety of different functions, such as antibiotic resistance, denitrification, N fixation, organic contaminant degradation, and sulfate reduction.

Results showed that reactors B and C grouped together, thus forming a separate cluster from reactors A, D and E. Based on gene clustering, twelve different groups were detected. Genes from clusters 3, 5, and 8 were detected in all wells. Whereas clusters 1, 2, 6, 7, 9, and 11 were detected in 2 or 3 of the reactors. Finally, some of the clusters were only detected in one reactor, and more specifically: cluster 4 in reactor E, cluster 10 in reactor A and cluster 12 in reactor C.

Table 1 – Gas production and coulombic efficiency in MEC reactors.

	H_2 (mL)	H_2 yield (mol H_2/$mol_{glucose}$)	CH_4 (mL)	CO_2 (mL)	Coulombic efficiency (%)
A	1.89 ± 0.86	0.78 + 0.36	5.61 ± 0.40	2.19 ± 0.24	59 ± 4
B	4.27 ± 1.14	1.67 + 0.47	5.28 ± 0.11	3.36 ± 0.16	61 ± 5
C	12.16 ± 1.05	5.01 + 0.43	4.83 ± 0.26	3.13 ± 0.22	65 ± 5
D	0.10 ± 0.09	0.04 + 0.03	3.71 ± 0.41	1.94 ± 0.26	45 ± 1
E	5.65 ± 2.57	2.33 + 1.06	4.57 ± 0.26	2.58 ± 0.21	61 ± 5

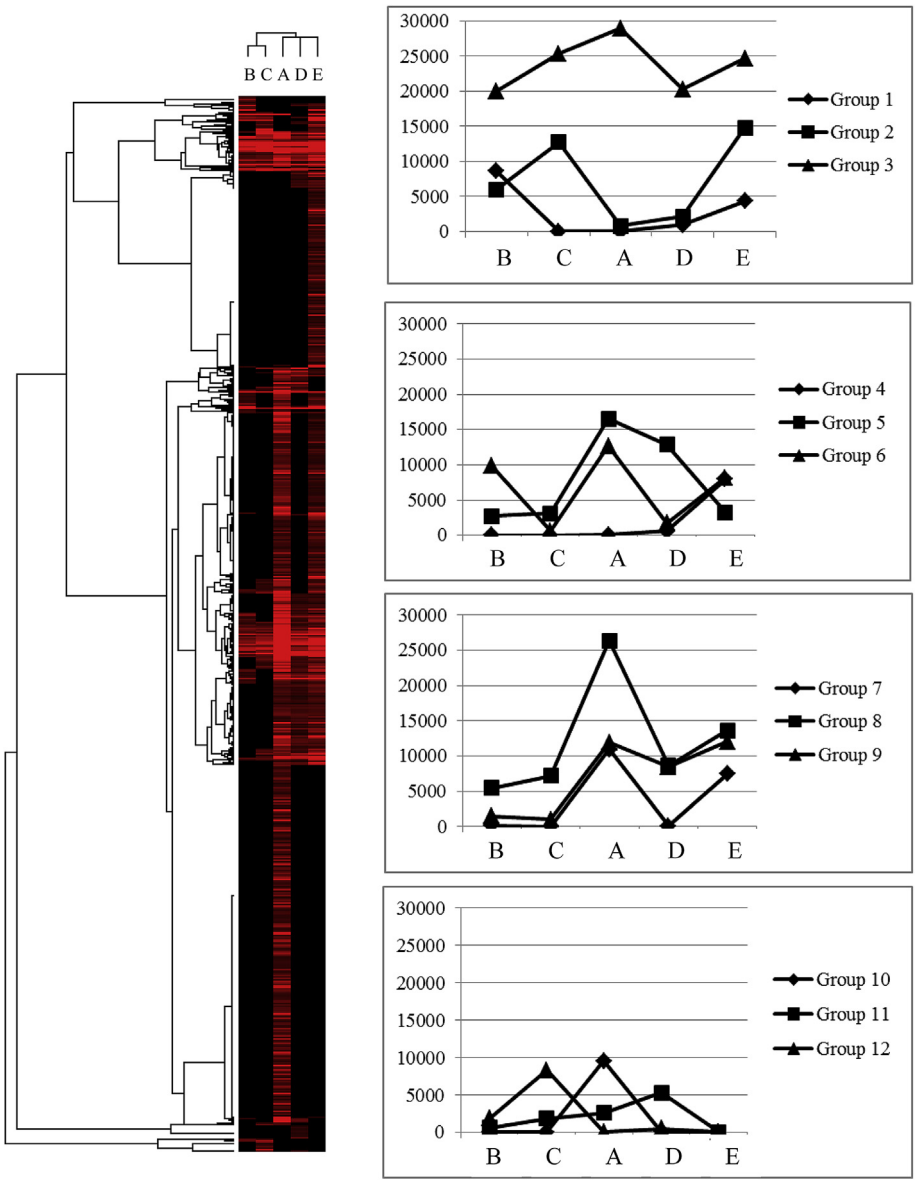

Fig. 1 – Hierarchical cluster analysis of all genes detected in all reactors. Signal intensities were averaged for replicate reactors. Results were generated in CLUSTER and visualized in TREEVIEW. Red indicates signal intensities above background and black indicates signals below background. Higher intensity reds indicate higher signal intensities. Graphs to the right indicate average signal intensities of each cluster. (For interpretation of the references to color in this figure legend, the reader is referred to the web version of this article.)

DCA was then used to further examine changes in the functional microbial community structure (Fig. 2). In DCA ordination plots, samples that are more similar are closer together, while those that are more different are further apart. The relatively small error bars indicate that replicate reactors had similar community structures. All the reactors separated well, with minimal overlap. As can be seen, reactor A was located furthest from the other reactors, thus indicating that it was the most dissimilar one. The other reactors were more similar but still distinct from each other. Reactors B and C were separated by axis 2, and were clearly distinct from reactors D, E and A (which distributed along axis 1). Dissimilarity testing with Adonis indicated that the communities from each reactor were significantly different from each other ($p = 0.001$).

3.4. *Relative abundance of functional genes*

To further examine differences in the microbial communities, the relative abundance of all functional gene groups was also considered (Fig. 3). While genes from all categories were detected in each reactor, there were differences in the relative abundance of gene groups between reactors. In accordance with the cluster analysis, reactors B and C had similar profiles, although gas production in these two reactors was quite different. Same situation was observed for reactors A and E.

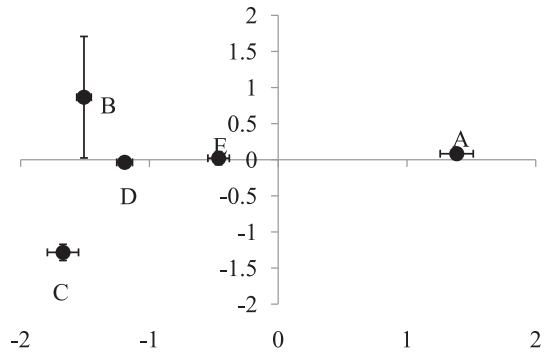

Fig. 2 – DCA of all genes detected by GeoChip. Letters indicate reactor name. Error bars are standard deviation of triplicate reactors.

On the other hand, reactors B and E had similar gas productions but relatively different profiles.

Overall, the most abundant functional genes were related to metal resistance, followed by organic remediation, antibiotic resistance and carbon degradation.

3.5. *Changes in individual functional gene groups*

To further investigate the differences in functional structure between reactors, individual gene groups were examined, based on clustering analysis.

3.5.1. *Carbon cycling*

While all reactors were fed with glucose as the sole carbon source, several genes involved in complex carbon degradation were detected, including genes for degradation of cellulose, hemicellulose, lignin, starch, pectin, and chitin (Fig. S2).

Genes for acetogenesis, degradation of cellulose, chitin, hemocellulose, lignin, starch, vanillin, and malate synthase were detected in all reactors. Carbon fixation genes were also detected, including genes for rubisco, carbon monoxide dehydrogenase, and propionyl-CoA carboxylase from a variety of different microorganisms (Fig. S3). A rubisco derived from an uncultured bacterium (gi157679123) was detected in all reactors. Propionyl-CoA carboxylase genes derived from *Roseiflexus* sp. (148657926), *Nitrobacter hamburgensis* (92117653), *Chloroflexus aggregans* (118045694), carbon monoxide dehydrogenase (CODH) from an uncultured bacterium (lab clone), and rubisco derived from an uncultured bacterium (224579026) were also detected in most of the reactors.

3.5.2. *Methane*

Nineteen genes involved in methane oxidation or methanogenesis were detected across all reactors (Fig. S4). Of these, four were for methane production (*mcrA*) and the remainder for methane oxidation (*pmoA* or *mmoX*). Most of the detected genes were from uncultured bacteria. *mcrA* was detected in most reactors, with the highest number being detected in reactor A, which showed the highest level of methane production, although this reactor also contained the highest number of methane oxidation genes.

3.5.3. *N cycling*

Genes involved in denitrification, N reduction, N fixation, ammonification, and nitrification were detected in all reactors (Fig. S5–S8). Most of the genes were detected in reactors A and E. The largest part of the denitrification and N fixation genes (*nirK*, *nirS*, *norB*, *narG*, *nosZ*) belonged to uncultured bacteria (Fig. S5). Sequences for *narG* (gi26278770, gi124488241) and *nirS* (57335474) were detected in all reactors. Sequences for N reduction (*nirA*, *nirB*, *nasA*, *nrfA*, *napA*) were mostly detected in reactor A. A *nrfA*, derived from *Desulfitobacterium hafniense*

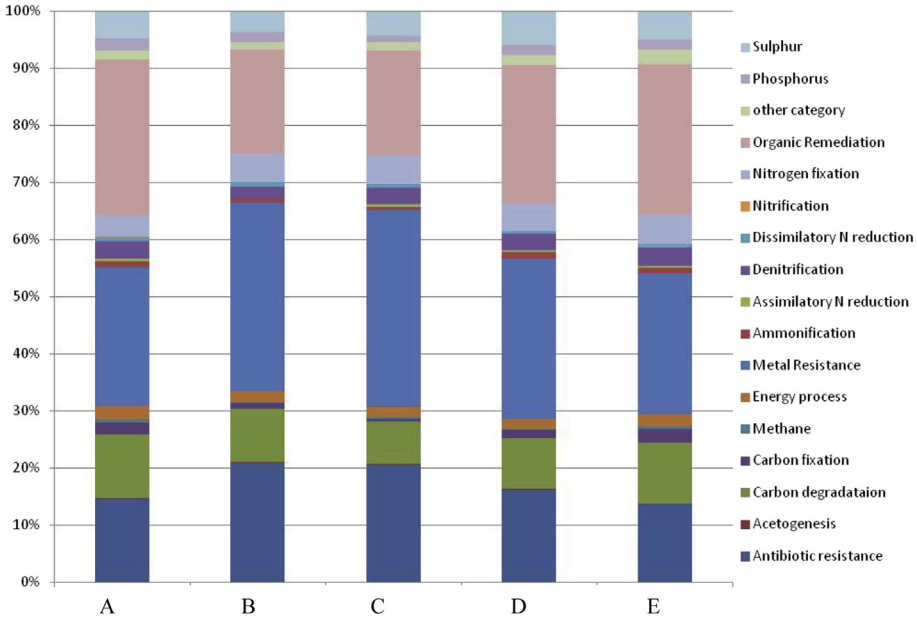

Fig. 3 – Relative abundance of all gene categories covered by the GeoChip. Abundance was calculated by dividing the total signal intensity of each gene category by the total signal intensity of all genes detected.

DCB-2 (gi109645564), and a *ureA*, derived from *Ralstonia pickettii* 12D (gi151575999), were detected in all reactors. Ammonification and nitrification genes (*ureC*, *amoA*, *hzo*, *gdh*, *hao*) were also detected in most reactors.

3.5.4. *Metal resistance*

A previous study of *Geobacter sulfurreducens*-MEC indicated an increase in transcription of several metal resistance genes, including efflux transporters for Cd, Co and Zn resistance [31]. In the present study, metal resistance was the most abundant functional gene group (see Fig. 3). Therefore, we decided to examine metal resistance genes more in detail. Genes for resistance to As (*arsB*, *arsC*), Cd (*cadA*, *cadBD*), Cd, Co, and Zn (*czcA*, *czcD*), Cr (*chrA*), Co (*corC*), Co and Ni (*cnrA*, *cnrC*), Cu (*copA*, *cueO*, *cusF*), Pb (*pbrA*, *pbrD*), Hg (*merA*, *merB*, *merP*, *merT*, *metC*), Ni (*nreB*), Ag (*silA*, *silC*, *silP*), Te (*tehB*, *terC*, *terD*, *terZ*), and Zn (*zitB*, *zntA*) were detected and most of these genes were found in all reactors, as can be seen in Fig. S9.

3.5.5. *Hydrogenases*

Hydrogenases catalyze the oxidation/reduction of H_2/H^+. As these enzymes are involved in the generation of H_2, we examined them more in detail. Twenty-nine hydrogenase genes were detected across all reactors, with 10 being detected in at least two replicate reactors (Fig. 4). It is worth noting that reactor C, which had the highest H_2 production rates, contained the fewest hydrogenases. Hydrogenases derived from *Dehalococcoides ethenogenes* 195 (57233678), *Desulfovibrio desulfuricans* subsp. desulfuricans (220904110), *Desulfovibrio fructosovorans* (186883006), *Shewanella baltica* OS223 (217498707), and *Rhodobacter sphaeroides* (126462908) were detected in all reactors. Hydrogenase genes are designed principally related to hydrogen generation (proton reduction) in GeoChip. However, their detection in the anode communities was assumed to contribute to proton reduction in fermentation process. But the fact was that the least hydrogenase genes were detected in reactor C with the highest hydrogen yield, indicating that hydrogen conversion would not be determined primarily by fermentation metabolism. Therefore, hydrogen production was significantly controlled by electron transporting process in MECs.

3.5.6. *Cytochromes*

In total, 105 cytochrome genes were detected in all reactors, with 32 being detected in at least two replicate reactors (Fig. 5). According to the hierarchical cluster analysis of cytochrome genes, reactor C resulted to be distinct from the other reactors. Only one cytochrome sequence, derived from *Geobacter metallireducens* GS-15 (78221556, involved in Fe(III) respiration), was detected in all reactors. Cytochromes derived from *Bradyrhizobium* sp. (146190249, involved in oxidation of organic contaminants) and *G. sulfurreducens* (39995384, *OmcA*/*MtrC*) were also detected in most reactors.

Several cytochrome *c* genes are known to be involved in electron transport mechanism in microbial fuel cells, including the outer membrane associated metal reductases, *OmcB* (*MtrC*) and *OmcA* [32]. In the present study *OmcA*/*MtrC* from *G. sulfurreducens* (39995699, 39997094, 39996436), *Shewanella sediminis*

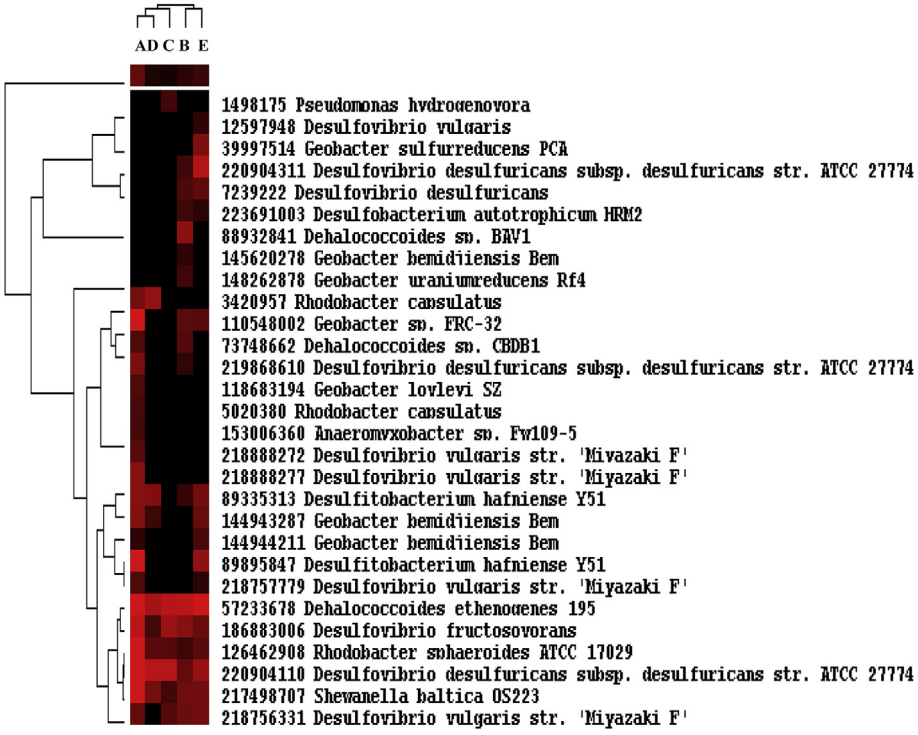

Fig. 4 – Hierarchical cluster analysis of hydrogenase genes. Signal intensities were averaged for replicate reactors. Results were generated in CLUSTER and visualized in TREEVIEW. Red indicates signal intensities above background and black indicates signals below background. Higher intensity reds indicate higher signal intensities. (For interpretation of the references to color in this figure legend, the reader is referred to the web version of this article.)

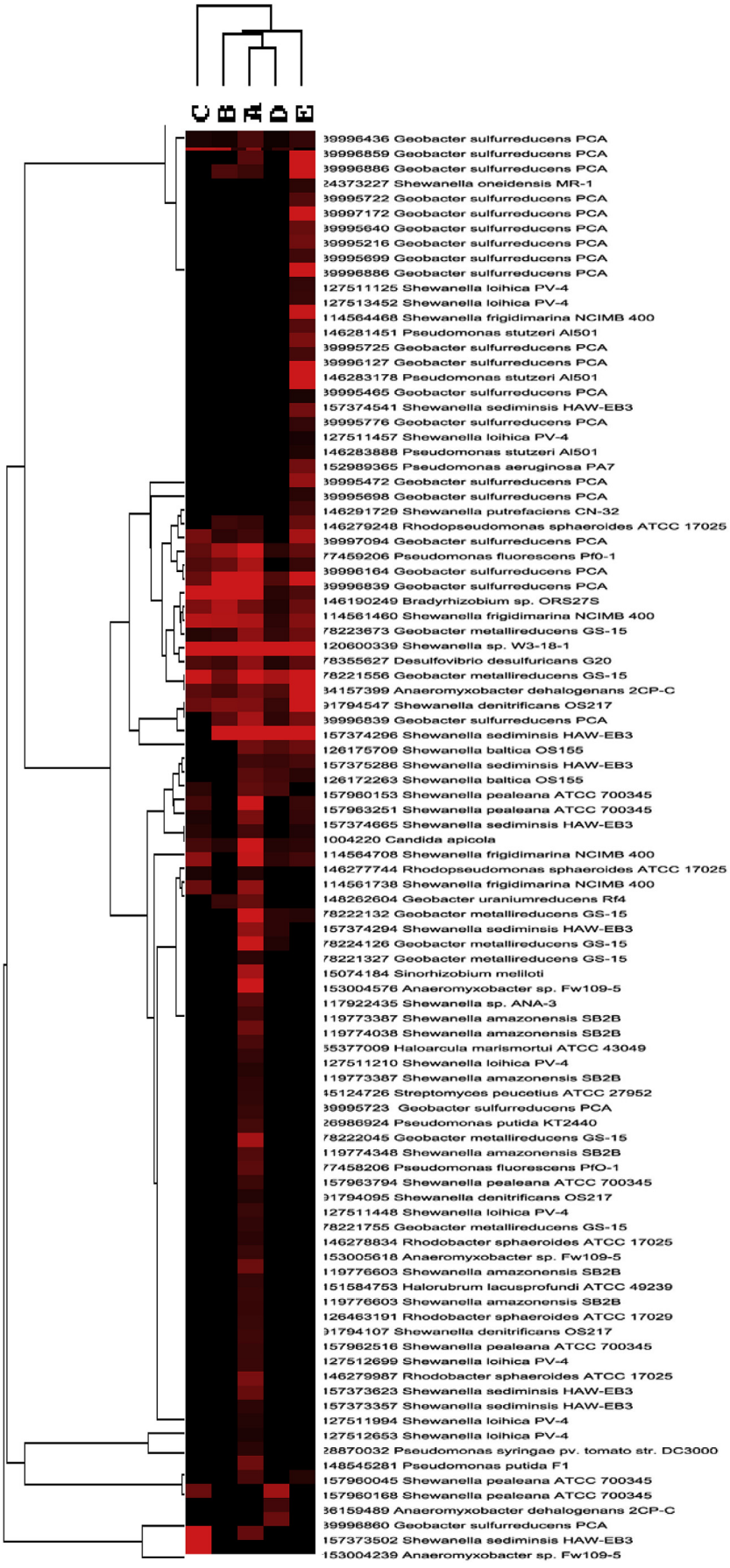
39996436 Geobacter sulfurreducens PCA
39996859 Geobacter sulfurreducens PCA
39996886 Geobacter sulfurreducens PCA
24373227 Shewanella oneidensis MR-1
39995722 Geobacter sulfurreducens PCA
39997172 Geobacter sulfurreducens PCA
39995640 Geobacter sulfurreducens PCA
39995216 Geobacter sulfurreducens PCA
39995699 Geobacter sulfurreducens PCA
39996886 Geobacter sulfurreducens PCA
127511125 Shewanella loihica PV-4
127513452 Shewanella loihica PV-4
114564468 Shewanella frigidimarina NCIMB 400
146281451 Pseudomonas stutzeri A1501
39995725 Geobacter sulfurreducens PCA
39996127 Geobacter sulfurreducens PCA
146283178 Pseudomonas stutzeri A1501
39995465 Geobacter sulfurreducens PCA
157374541 Shewanella sediminsis HAW-EB3
39995776 Geobacter sulfurreducens PCA
127511457 Shewanella loihica PV-4
146283888 Pseudomonas stutzeri A1501
152989365 Pseudomonas aeruginosa PA7
39995472 Geobacter sulfurreducens PCA
39995698 Geobacter sulfurreducens PCA
146291729 Shewanella putrefaciens CN-32
146279248 Rhodopseudomonas sphaeroides ATCC 17025
39997094 Geobacter sulfurreducens PCA
77459206 Pseudomonas fluorescens Pf0-1
39996164 Geobacter sulfurreducens PCA
39996839 Geobacter sulfurreducens PCA
146190249 Bradyrhizobium sp. ORS27S
114561460 Shewanella frigidimarina NCIMB 400
78223673 Geobacter metallireducens GS-15
120600339 Shewanella sp. W3-18-1
78355627 Desulfovibrio desulfuricans G20
78221556 Geobacter metallireducens GS-15
34157399 Anaeromyxobacter dehalogenans 2CP-C
91794547 Shewanella denitrificans OS217
39996839 Geobacter sulfurreducens PCA
157374296 Shewanella sediminsis HAW-EB3
126175709 Shewanella baltica OS155
157375286 Shewanella sediminsis HAW-EB3
126172263 Shewanella baltica OS155
157960153 Shewanella pealeana ATCC 700345
157963251 Shewanella pealeana ATCC 700345
157374665 Shewanella sediminsis HAW-EB3
1004220 Candida apicola
114564708 Shewanella frigidimarina NCIMB 400
146277744 Rhodopseudomonas sphaeroides ATCC 17025
114561738 Shewanella frigidimarina NCIMB 400
148262604 Geobacter uraniumreducens Rf4
78222132 Geobacter metallireducens GS-15
157374294 Shewanella sediminsis HAW-EB3
78224126 Geobacter metallireducens GS-15
78221327 Geobacter metallireducens GS-15
15074184 Sinorhizobium meliloti
153004576 Anaeromyxobacter sp. Fw109-5
117922435 Shewanella sp. ANA-3
119773387 Shewanella amazonensis SB2B
119774038 Shewanella amazonensis SB2B
55377009 Haloarcula marismortui ATCC 43049
127511210 Shewanella loihica PV-4
119773387 Shewanella amazonensis SB2B
45124726 Streptomyces peucetius ATCC 27952
39995723 Geobacter sulfurreducens PCA
26986924 Pseudomonas putida KT2440
78222045 Geobacter metallireducens GS-15
119774348 Shewanella amazonensis SB2B
77458206 Pseudomonas fluorescens Pf0-1
157963794 Shewanella pealeana ATCC 700345
91794095 Shewanella denitrificans OS217
127511448 Shewanella loihica PV-4
78221755 Geobacter metallireducens GS-15
146278834 Rhodobacter sphaeroides ATCC 17025
153005618 Anaeromyxobacter sp. Fw109-5
119776603 Shewanella amazonensis SB2B
151584753 Halorubrum lacusprofundi ATCC 49239
119776603 Shewanella amazonensis SB2B
126463191 Rhodobacter sphaeroides ATCC 17029
91794107 Shewanella denitrificans OS217
157962516 Shewanella pealeana ATCC 700345
127512699 Shewanella loihica PV-4
146279987 Rhodobacter sphaeroides ATCC 17025
157373623 Shewanella sediminsis HAW-EB3
157373357 Shewanella sediminsis HAW-EB3
127511994 Shewanella loihica PV-4
127512653 Shewanella loihica PV-4
28870032 Pseudomonas syringae pv. tomato str. DC3000
148545281 Pseudomonas putida F1
157960045 Shewanella pealeana ATCC 700345
157960168 Shewanella pealeana ATCC 700345
36159489 Anaeromyxobacter dehalogenans 2CP-C
39996860 Geobacter sulfurreducens PCA
157373502 Shewanella sediminsis HAW-EB3
153004239 Anaeromyxobacter sp. Fw109-5

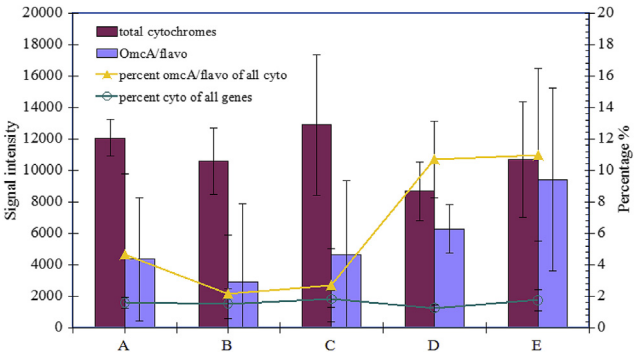

Fig. 6 – Abundance of cytochrome genes detected in the 5 reactors by GeoChip. Green line indicates the relative abundance of total cytochrome genes (as % of all genes), while the yellow line shows the relative abundance of cytochromes known to be involved in electron transport in MECs (as % of all cytochrome genes). Bars indicate the total signal intensity of total cytochromes (in purple) and of those involved in electron transport (in blue), respectively. (For interpretation of the references to color in this figure legend, the reader is referred to the web version of this article.)

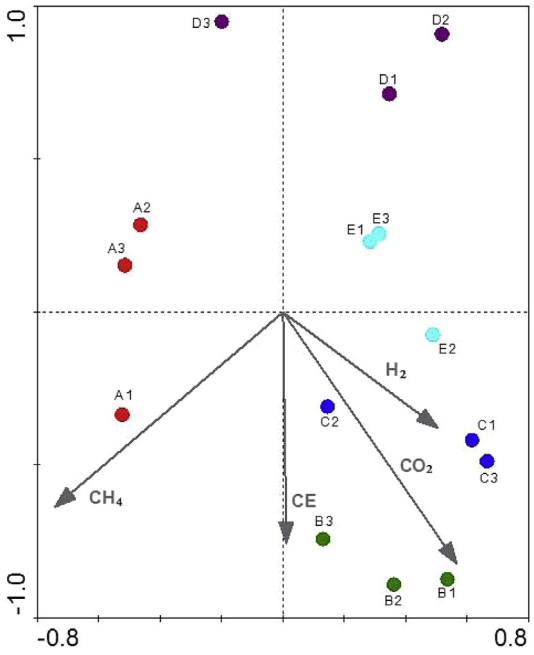

Fig. 7 – CCA of all genes detected by GeoChip and reactor productivity values. Circles indicate reactors, letters and numbers indicate reactor names; arrows indicate productivity measures (Factors: H_2 for hydrogen, CO_2 for carbon dioxide, and CH_4 for methane, CE for coulombic efficiency).

(157374666, 157374665), *Shewanella oneidensis* (24373227), *Shewanella amazonensis* (119774348), *Shewanella loihica* (127513452), and *Shewanella pealeana* (157960153, 157962516) were detected in the reactors. Flavocytochromes (which act as electron shuttles) from *S. baltica* (126172505, 126172508) and *S. loihica* (127511210) were also detected. Other cytochrome genes included *DmsE* (DMSO reduction), *NapB*, *NapC* (both for nitrate reduction), *P450* (oxidation of organic contaminants), *LivK* (manganese oxidation), *CoxB* (oxidative phosphorylation) and others involved in metal reduction, aerobic respiration, sulfite oxidation, and cytochrome assembly.

A similar relative abundance of cytochrome genes (% of total gene abundance) was detected across all reactors (ranging from 1.3 to 1.8%; Fig. 6). Reactor C, which had the highest H_2 production, showed a higher (total) amount of cytochrome genes, although the abundance of cytochrome genes involved in electron transport (including outer membrane associated metal reductases and flavocytochromes) were higher in reactors D and E.

Since exoelectrogenic bacteria are often capable of metal reduction, metal reducing strains were also further examined. Cytochrome *c* genes derived from 28 different microbial strains were detected in the reactors (Fig. S10). Among these, *Anaeromyxobacter dehalogenans* 2CP-C, *Bradyrhizobium* sp. ORS278, *D. desulfuricans* G20, *G. metallireducens* GS-15, *G. sulfurreducens* PCA, *Shewanella denitrificans* OS217, *Shewanella frigidimarina* NCIMB 400, *S. sediminis* HAW-EB3, and *Shewanella* sp. were detected in all reactors.

3.6. *Relationship between gas production and microbial community structure*

Canonical Correspondence Analysis (CCA) was used to determine how gas reactor performance variables (gas production and coulombic efficiency) were affected by the community structure. Coulombic efficiency referred to the recovery of electrons, defined as the fraction of electrons recovered as current versus that present in the starting organic matter. Variance inflation factors (VIFs) for all variables examined were less than 4.5, indicating that the variables were independent. The model was significant ($p = 0.002$) and explained 30.4% of the variation (sum of all Eigenvalues, 1.444) (Fig. 7). The first canonical axis was positively correlated with H_2 and CO_2, and negatively correlated with CH_4. The second canonical axis was negatively correlated with CO_2, coulombic efficiency and methane, and to a lesser extent also with H_2. Reactors B and C (but also E) were positively correlated with CO_2 and H_2, with CO_2 showing the strongest correlation. Reactor A was positively correlated with CH_4, while reactor C (and to a lesser extent also reactor B) was positively correlated with coulombic efficiency.

Further, Variance Partitioning Analysis (VPA) [33,34] was performed to better understand how much each of the

Fig. 5 – Hierarchical cluster analysis of cytochrome genes. Signal intensities were averaged for replicate reactors. Results were generated in CLUSTER and visualized in TREEVIEW. Red indicates signal intensities above background and black indicates signals below background. Higher intensity reds indicate higher signal intensities. (For interpretation of the references to color in this figure legend, the reader is referred to the web version of this article.)

performance variables were influenced by the community structure. When CH_4, CO_2, and coulombic efficiency were held constant, there was only a weak correlation ($p = 0.082$) between H_2 production and the community structure. When H_2 and coulombic efficiency were held constant, CH_4 and CO_2 showed a significant correlation ($p = 0.002$). H_2 was able to independently explain 7.6% of the variation observed, CH_4 and CO_2 independently explained 23.8%, and coulombic efficiency, while not significant ($p = 0.150$), was able to independently explain 7.9%. There was some interaction between H_2, CH_4 and CO_2 (4.5%), and between CH_4 and CO_2 and coulombic efficiency (1.7%) as well. Over half of the variation (55.9%) remained unexplained.

4. Discussion

4.1. H_2 production in MECs

All of the MEC reactors examined in this study were able to produce H_2 at room temperature with 1 g/L glucose as the only added carbon source. Glucose fermentation produces several acids (e.g., acetic and lactic acids), which can, in turn, generate additional H_2 in the MEC.

Even though all reactors were inoculated with the same starting material and were treated in the same way (same parameters, carbon source and medium), the efficiency of H_2 production and total yield varied greatly between reactors (from 0.10 to 12.2 mL H_2, with a yield ranging from 0.04 to 5.01 mol $H_2/mol_{glucose}$), thus implying a large variability in the biofilm formation process. This further suggests that anode community development might be a very stochastic process, not directly associated to the controlled parameters, and that an enrichment phase might be useful (especially when using a complex inoculum, such as wastewater).

Clearly there could be several reasons for differences in the H_2 production. Hydrogenases catalyze the reversible oxidation of H_2; they can produce H_2 or use it. Several hydrogenases were detected in all reactors, but detection of the genes does not indicate whether the reaction is catalyzing H_2 production or utilization. Moreover, methane production can also consume H_2 [35]. This methane is most likely obtained from hydrogenotrophic methanogenesis, since there was insufficient time to form a methanogenic biofilm [36]. In our reactors, higher methane levels tended to correlate with lower H_2 levels (as confirmed by the Canonical Correspondence Analysis), although this was not always the case, probably because H_2 can also be consumed by chemolithotrophic bacteria [37]. The presence of H_2-consuming bacteria might also explain why, despite the interesting H_2 yield (about 5 mol $H_2/mol_{glucose}$), a previous study by Cheng and Logan [19] reported performances of up to 8.55 mol $H_2/mol_{glucose}$ (while methane was detected only in traces), at an applied voltage of 0.6 V.

Despite the differences among the reactors A–E, these results showed that wastewater represents a suitable inoculum for effective H_2 production with MEC technology. However a suitable treatment to inhibit the growth of H_2-consuming bacteria would clearly further enhance yields. In fact, while the use of single-chamber reactors allows for a simple reactor design, on the other hand we must also consider that the lack of membrane can reduce H_2 recoveries, due to H_2 consumption by microorganisms in the wastewater [35].

4.2. Functional gene diversity

While reactors in this study were fed only glucose, the functional diversity was quite high in all reactors (in accordance with Liu et al. [18], who used acetate as the sole carbon), both in terms of diversity indices and number of different functional gene categories detected. Genes from all major functional categories were detected in all reactors, indicating that the microbial communities were able to perform a large variety of functions. This was expected, due to the use of wastewater as inoculum.

According to the Canonical Correspondence Analysis, used to determine how gas reactor performance variables were affected by the community structure, reactors B, C and E positively correlated to H_2. Reactors B and C also positively correlated to coulombic efficiency. However, we did not observe a correlation between diversity and H_2 production. In fact, the reactor with the highest H_2 production (reactor C) had the lowest diversity, while another reactor with a similar diversity performed only moderate level of H_2 production. This suggests that variability was not necessarily (only) related to the presence of electrochemically active bacteria, as a fraction of the biofilm can be formed by non-exoelectrogens, such as fermentation and or symbiotic relationships with other bacteria [38]. This also suggests that probably some important "non-exoelectrogenic" functions, involved in H_2 production (such as formate-liase enzymes), were not taken into account.

Clearly, the presence of H_2-consuming bacteria might also add an important contribution to the diversity of the diversity of the community: in fact, according to the Variance Partitioning Analysis (VPA), variability of methane producers explained up to 24% of the variation, against only 7.6% for H_2. This might explain why H_2 production was not associated to biodiversity, since a large part of variability was associated to methane producing organisms.

In any case, as already mentioned, differences in reactor performance could also be linked to a different development of the exoelectrogenic bacterial community among the different biofilms, as well as to the different microbe's position within the biofilm itself, thus underlining the importance of biofilm structure, such as stratification of functional groups [38].

4.3. Key microbial populations involved in H_2 production

The overall community structure was fairly different between reactors (Figs. 2, 3 and 7), and there were distinct differences which may help identifying populations important for (or detrimental to) overall H_2 production.

It is well known that specific cytochromes are essential [39,40] for bacteria, such as *Shewanella* [32] and *Geobacter* strains [31], to extracellularly transfer electrons to the electrode. *Shewanella*, for instance, is able to transfer electrons to the anode via the multiheme *c*-type cytochromes *MtrC* (*OmcB*) and *OmcA* [32]. These cytochromes were detected in all reactors. Other cytochrome genes derived from several known exoelectrogenic genera, including *Anaeromyxobacter*, *Desulfovibrio* [41], *Geobacter* [42], and *Shewanella* [43] were also

detected. The same genera were previously detected in MEC reactors with acetate as the sole carbon source [18]. Other functional genes from genera known to be exoelectrogens, such as *Clostridium*, *Desulfovibrio*, *Escherichia*, *Geobacter*, *Pseudomonas*, *Rhodopseudomonas*, and *Shewanella* spp. were present in all reactors examined in this study. In addition, flavins, which can act as electron shuttles [32], were also detected. The presence of these functional genes explains the ability of all reactors to produce H_2.

Clearly, as already mentioned, methane production is still a problem in MEC's with mixed cultures [44], because the metabolism of methanogens can decrease the amount of H_2 detected and/or produced, either through H_2 consumption to produce methane or substrate consumption. As such, methods to reduce the amount of methane produced in reactors are desirable to increase H_2 yields [35]. In fact, reactors with the highest H_2 production had the least amount of methanogens.

Another population of interest consists of hydrogenase containing bacteria, since they can either use or produce H_2. Compared with the other reactors, Reactor C had considerably higher exoelectrogenic bacteria (such as *Shewanella*, *Geobacter*), less methanogens and less hydrogen-utilizing bacteria. This is consistent with observations that the highest hydrogen yield was obtained in this reactor, and confirms the importance of dissimilatory metal-reducing bacteria such as *Geobacter* and *Shewanella* species [38].

4.4. MECs and wastewater treatment

In the present study, many carbon degradation and contaminant degradation genes were detected, suggesting that a wide range of carbon sources could be utilized by the microbial community. In addition, several functional capabilities, found in the reactors investigated in this study, would be useful in wastewater treatment. Organic contaminant degradation related genes can remove contaminants by metabolizing them to nontoxic substrates, which can then be utilized by other microorganisms. Toxic metals can be reduced by microorganisms, to remove them from solution, or could be sequestered by excreted substances such as sulfide from sulfate-reducing bacteria. Genes for degradation of herbicides and pesticides, solvents, and chlorinated compounds were detected. Phosphorus utilization, sulfate reduction, and nitrogen reduction genes were also detected, which would be all useful in wastewater treatment [45–47].

For this reason, the selected microbial community might represent a suitable inoculum not only for H_2 production, but also for a concomitant effective wastewater treatment.

In fact, wastewater still contains organic material that can provide suitable nutrition for both, exoelectrogenic and non-exoelectrogenic microbes. The latter could then be helpful to remove contaminants, such as toxic compounds (present in wastewater) that must be treated prior to disposal.

It is worth noting that successful biological H_2 production depends on the overall performance (results of interactions) of the bacterial community in the reactor. Therefore, metabolic cooperation within the bacterial community may provide useful combinations of metabolic pathways for the processing of complex waste material (and the degradation of impurities and/or inhibitors), thereby supporting a more efficient decomposition of substrate [48–51].

Therefore, the great advantage of coupling wastewater treatment with MECs would be that extra hydrogen is recovered, while the wastewater is treated by removing organic matter and contaminants through oxidation [35,45–47].

5. Conclusion

In this study we have developed an effective community for hydrogen production, able to produce up to 5.01 mol H_2/mol$_{glucose}$ (reactor C), using wastewater as inoculum. Maximum coulombic efficiency reached 65 (±5)%. GeoChip-based metagenomic analysis allowed to observe a large variety of microbial functional genes, with approximately 2000 different functional genes detected across all reactors. H_2 production correlated with the community structure, but not with the diversity. The most abundant functional genes detected were related to metal resistance, followed by organic remediation, antibiotic resistance and carbon degradation. Reactor C, with the best performance, had considerably higher exoelectrogenic bacteria (e.g. *Shewanella*, *Geobacter*), less methanogens and less hydrogen-utilizing bacteria, compared with the others. These results suggest that wastewater represents a suitable inoculum for effective H_2 production with MEC technology, however a suitable treatment to inhibit the growth of H_2-consuming bacteria (such as methanogens) would clearly allow to further enhance the yields. Further, these results also showed that GeoChip can provide useful information for the characterization of complex microbial communities and that MEC can be considered a promising technology to produce hydrogen from wastewater.

Acknowledgments

This research was supported by National Natural Science Foundation of China (NSFC, Grant No. 51111140388, No. 51208496), by Science Fund for Creative Research Groups of the National Natural Science Foundation of China (Grant No. 51121062) by China Postdoctoral Science Foundation (No. 2012M510574 and No. 2013T60182). This work was also supported by the State Key Laboratory of Urban Water Resource and Environment (Grant No. 2010DX11 and No. 2011TS09).

Appendix A. Supplementary data

Supplementary data related to this article can be found at http://dx.doi.org/10.1016/j.ijhydene.2014.01.001.

REFERENCES

[1] Levin DB, Pitt L, Love M. Biohydrogen production: prospects and limitations to practical application. Int J Hydrogen Energy 2004;29(2):173–85.

[2] Kapdan IK, Kargi F. Bio-hydrogen production from waste materials. Enzym Microb Technol 2006;38:569–82.
[3] Dharmadi Y, Murarka A, Gonzalez R. Anaerobic fermentation of glycerol by *Escherichia coli*: a new platform for metabolic engineering. Biotechnol Bioeng 2006;94(5):821–9.
[4] DOE. Biomass to biofuels workshop. In: From biomass to biofuels: a roadmap to the energy future. December 7–9, 2005 2006. Rockville, MD.
[5] Balat M, Balat H. Recent trends in global production and utilization of bioethanol fuel. Appl Energy 2009;86:2273–82.
[6] Qiu H, Huang J, Yang J, Rozelle S, Zhang Y, Zhang Y, et al. Bioethanol development in China and the potential impacts on its agricultural economy. Appl Energy 2010;87:76–83.
[7] Liu H, Gort S, Logan BE. Electrochemically assisted microbial production of hydrogen from acetate. Environ Sci Technol 2005;39:4317–20.
[8] Sun MG, Sheng L, Zhang C, Xia Z, Mu X, Liu H, et al. An MEC-MCF-coupled system for biohydrogen production from acetate. Environ Sci Technol 2008;42:8095–100.
[9] Esper B, Badura A, Rogner M. Photosynthesis as a power supply for (bio-) hydrogen production. Trends Plant Sci 2006;11:543–9.
[10] Li CL, Fang HHP. Fermentative hydrogen production from wastewater and solid wastes by mixed cultures. Crit Rev Environ Sci Technol 2007;37:1–39.
[11] Hoffmann P. Tomorrow's energy—hydrogen, fuel cells and the prospects for a cleaner planet. Cambridge, MA: MIT Press; 2001.
[12] Das D, Veziroglu TN. Hydrogen production by biological processes: a survey of literature. Int J Hydrogen Energy 2001;26(1):13–28.
[13] Akkerman I, Janssen M, Rocha J, Wijffels RH. Photobiological hydrogen production: photochemical efficiency and bioreactor design. Int J Hydrogen Energy 2002;27:1195–208.
[14] Krupp M, Widmann R. Biohydrogen production by dark fermentation: experiences of continuous operation in large lab scale. Int J Hydrogen Energy 2009;34:4509–16.
[15] Logan BE. Extracting hydrogen electricity from renewable resources. Environ Sci Technol 2004;38(9):160–7.
[16] Call DF, Logan BE. Hydrogen production in a single chamber microbial electrolysis cell lacking a membrane. Environ Sci Technol 2008;42:3401–6.
[17] Selembo PA, Merrill MD, Logan BE. The use of stainless steel and nickel alloys as low-cost cathodes in microbial electrolysis cells. J Power Sources 2009;190(2):271–8.
[18] Liu W, Wang A, Cheng S, Logan BE, Yu H, Deng Y, et al. GeoChip-based functional gene analysis of anodophilic communities in microbial electrolysis cells under different operational modes. Environ Sci Technol 2010;44:7729–35.
[19] Cheng S, Logan BE. Sustainable and efficient biohydrogen production via electrohydrogenesis. Proc Natl Acad Sci U S A 2007;104:18871–3.
[20] Chen G, Choi S, Lee T, Lee G, Cha J, Kim C. Application of biocathode in microbial fuel cells: cell performance and microbial community. Appl Microbiol Biotechnol 2008;79:379–88.
[21] Chae K, Choi M, Lee J, Kim K, Kim IS. Effect of different substrates on the performance, bacterial diversity, and bacterial viability in microbial fuel cells. Bioresour Technol 2009;100:3518–25.
[22] Chung K, Okabe S. Continuous power generation and microbial community structure of the anode biofilms in a three-stage microbial fuel cell system. Appl Microbiol Biotechnol 2009;83:9635–977.
[23] Kim GT, Webster G, Wimpenny JWT, Kim BH, Kim HJ, Weightman AJ. Bacterial community structure, compartmentalization and activity in a microbial fuel cell. J Appl Microbiol 2006;101:698–710.
[24] Zuo Y, Xing D, Regan JM, Logan BE. Isolation of the exoelectrogenic bacterium *Ochrobactrum anthropi* YZ-1 by using a U-tube microbial fuel cell. Appl Environ Microbiol 2008;74:3130–7.
[25] He Z, Deng Y, Van Nostrand JD, Tu Q, Xu M, Hemme CL, et al. GeoChip 3.0 as a high-throughput tool for analyzing microbial community composition, structure, and functional activity. ISME J 2010;4(9):1167–79.
[26] Zhou J, Bruns MA, Tiedje JM. DNA recovery from soils of diverse composition. Appl Environ Microbiol 1996;62:316–22.
[27] Wu L, Liu X, Schadt CW, Zhou J. Microarray-based analysis of subnanogram quantities of microbial community DNAs by using whole-community genome amplification. Appl Environ Microbiol 2006;72:4931–41.
[28] Van Nostrand JD, Wu WM, Wu L, Deng Y, Carley Y, Carroll S, et al. GeoChip-based analysis of functional microbial communities during the reoxidation of a bioreduced uranium-contaminated aquifer. Environ Microbiol 2009;11:2611–26.
[29] Wu L, Liu X, Fields MW, Thompson DK, Bagwell CE, Tiedje JM, et al. Microarray-based whole-genome hybridization as a tool for determining procaryotic species relatedness. ISME J 2008;2:642–55.
[30] Casgrain P, Legendre P. The R package for multivariate and spatial analysis, version 4.0 (development release 6); 2001. In Montreal, U. d., Ed. Quebec, Canada.
[31] Holmes DE, Chaudhuri SK, Nevin KP, Mehta T, Methe BA, Liu A, et al. Microarray and genetic analysis of electron transfer to electrodes in *Geobacter sulfurreducens*. Environ Microbiol 2006;8:1805–15.
[32] Fredrickson JK, Romine MF, Beliaev AS, Auchtung JM, Driscoll ME, Gardner TS, et al. Towards environmental systems biology of *Shewanella*. Nat Microbiol Rev 2008;6:592–603.
[33] Økland RH, Eilertsen O. Canonical correspondence analysis with variation partitioning: some comments and an application. J Veg Sci 1994;5(1):117–26.
[34] Ramette A, Tiedje JM. Multiscale responses of microbial life to spatial distance and environmental heterogeneity in a patchy ecosystem. Proc Natl Acad Sci 2007;104(8):2761–6.
[35] Wagner RC, Regan JM, Oh SE, Zuo Y, Logan BE. Hydrogen and methane production from swine wastewater using microbial electrolysis cells. Water Res 2009;43:1480–8.
[36] Wang A, Liu W, Cheng S, Xing D, Zhou J, Logan BE. Source of methane and methods to control its formation in single chamber microbial electrolysis cells. Int J Hydrogen Energy 2009;34:3653–8.
[37] Sørensen J, Christensen D, Jørgensen BB. Volatile fatty acids and hydrogen as substrates for sulfate-reducing bacteria in anaerobic marine sediment. Appl Environ Microbiol 1981;42(1):5–11.
[38] Logan BE, Regan JM. Microbial fuel cells: challenges and applicationsIntroduction to the special section on microbial fuel cells. Environ Sci Technol 2006;40(17):5172–80.
[39] Oh SB, Min B, Logan BE. Cathode performance as a factor in electricity generation in microbial fuel cells. Environ Sci Technol 2004;38:4900–4.
[40] Lovley DR. The microbe electric: conversion of organic matter to electricity. Curr Opin Biotechnol 2008;19(6):564–71.
[41] Cooney MJ, Roschi E, Marison IW, Comninellis C, von Stockar U. Physiologic studies with the sulfate-reducing bacterium *Desulfovibrio desulfuricans*: evaluation for use in a biofuel cell. Enzyme Microb Technol 1996;18(5):358–65.
[42] Bond DR, Lovley DR. Electricity production by *Geobacter sulfurreducens* attached to electrodes. Appl Environ Microbiol 2003;69(3):1548–55.
[43] Gorby YA, Yanina S, McLean JS, Rosso KM, Moyles D, Dohnalkova A, et al. Electrically conductive bacterial

nanowires produced by *Shewanella oneidensis* strain MR-1 and other microorganisms. Proc Natl Acad Sci U S A 2006;103(30):11358–63.

[44] Lalaurette E, Thammannagowda S, Mohagheghi A, Maness PC, Logan BE. Hydrogen production from cellulose in a two-stage process combining fermentation and electrohydrogenesis. Int J Hydrogen Energy 2009;34(15):6201–10.

[45] Gil-Carrera L, Escapa A, Mehta P, Santoyo G, Guiot SR, Morán A, et al. Microbial electrolysis cell scale-up for combined wastewater treatment and hydrogen production. Bioresour Technol 2013;130:584–91.

[46] Tuna E, Kargi F, Argun H. Hydrogen gas production by electrohydrolysis of volatile fatty acid (VFA) containing dark fermentation effluent. Int J Hydrogen Energy 2008;34:262–9.

[47] Rabaey K, Rodriguez J, Blackall L, Keller J, Gross P, Batstone D, et al. Microbial ecology meets electrochemistry: electricity-driven and driving communities. ISME J 2007;1:9–18.

[48] Varrone C, Rosa S, Fiocchetti F, Giussani B, Izzo G, Marone A, et al. Enrichment of activity sludge for enhanced hydrogen production from crude glycerol. Int J Hydrogen Energy 2013;38:1319–31.

[49] Marone A, Massini G, Patriarca C, Signorini A, Varrone C, Izzo G. Hydrogen production from vegetable waste by bioaugmentation of indigenous fermentative communities. Int J Hydrogen Energy 2012;37(7):5612–22.

[50] Sarma SJ, Brar SK, Sydney EB, Le Bihan Y, Buelna G, Soccol CR. Microbial hydrogen production by bioconversion of crude glycerol: a review. Int J Hydrogen Energy 2012;37:6473–90.

[51] Hung CH, Chang YT, Chang YJ. Roles of microorganisms other than *Clostridium* and *Enterobacter* in anaerobic fermentative biohydrogen production systems: a review. Bioresour Technol 2011;102:8437–44.